

Exact explicit solitary wave and periodic wave solutions and their dynamical behaviors for the Schamel-Korteweg-de Vries equation

Bin He(何斌) and Qing Meng(蒙清)

Citation: Chin. Phys. B, 2021, 30 (**6**): 060201. DOI: 10.1088/1674-1056/abd7d1
Journal homepage: http://cpb.iphy.ac.cn; http://iopscience.iop.org/cpb

What follows is a list of articles you may be interested in

High-order rational solutions and resonance solutions for a (3+1)-dimensional Kudryashov-Sinelshchikov equation

Yun-Fei Yue(岳云飞), Jin Lin(林机), and Yong Chen(陈勇)
Chin. Phys. B, 2021, 30 (**1**): 010202. DOI: 10.1088/1674-1056/abb3f3

Dynamical analysis for hybrid virus infection system in switching environment

Dong-Xi Li(李东喜), Ni Zhang(张妮)
Chin. Phys. B, 2020, 29 (**9**): 090201. DOI: 10.1088/1674-1056/ab8c3f

Dynamical behaviors of traveling wave solutions to a Fujimoto-Watanabe equation

Zhen-Shu Wen(温振庶), Li-Juan Shi(师利娟)
Chin. Phys. B, 2018, 27 (**9**): 090201. DOI: 10.1088/1674-1056/27/9/090201

Reweighted ensemble dynamics simulations: Theory, improvement, and application

Gong Lin-Chen, Zhou Xin, Ouyang Zhong-Can
Chin. Phys. B, 2015, 24 (**6**): 060202. DOI: 10.1088/1674-1056/24/6/060202

Complex dynamical behaviors of compact solitary waves in the perturbed mKdV equation

Yin Jiu-Li, Xing Qian-Qian, Tian Li-Xin
Chin. Phys. B, 2014, 23 (**8**): 080201. DOI: 10.1088/1674-1056/23/8/080201

Exact explicit solitary wave and periodic wave solutions and their dynamical behaviors for the Schamel–Korteweg–de Vries equation*

Bin He(何斌) and Qing Meng(蒙清)†

College of Mathematics and Statistics, Honghe University, Mengzi 661100, *China*

(Received 19 November 2020; revised manuscript received 28 December 2020; accepted manuscript online 4 January 2021)

The Schamel–Korteweg–de Vries equation is investigated by the approach of dynamics. The existences of solitary wave including ω-shape solitary wave and periodic wave are proved via investigating the dynamical behaviors with phase space analyses. The sufficient conditions to guarantee the existences of the above solutions in different regions of the parametric space are given. All possible exact explicit parametric representations of the waves are also presented. Along with the details of the analyses, the analytical results are numerically simulated lastly.

Keywords: Schamel–Korteweg–de Vries equation, dynamical behavior, solitary wave solution, periodic wave solution

PACS: 02.30.Hq, 02.30.Oz, 04.20.Jb **DOI:** 10.1088/1674-1056/abd7d1

1. Introduction

The Schamel–Korteweg–de Vries (Schamel-KdV) equation[1–18] can be written as

$$u_t + (\alpha u^{\frac{1}{2}} + \beta u)u_x + \delta u_{xxx} = 0, \quad \beta, \delta \neq 0, \tag{1}$$

where α, β and δ are constants and u is the wave potential, which arises in the study of ion acoustic solitons in plasma physics when electron trapping is present, and also it governs the electrostatic potential for a certain electron distribution in velocity space.[1,2] We mention that Eq. (1) reduces to the well-known KdV equation[3,4] when $\alpha = 0$ and reduces to the Schamel equation[5–7] when $\beta = 0$. It is known that the KdV equation has other kinds of explicit solutions, particularly rational solutions,[8] which provide better approximations to real physical nonlinear waves in terms of the complexity and computational time. More generally, lump solutions could exist in the Kadomtsev–Petviashvili equation[9] and other (2+1)-generalizations of the KdV equation.[10] Due to the wide range of applications of Eq. (1), it is important to find its new exact wave solutions. Khater *et al.*[11] obtained the periodic wave solutions using the F-expansion method. Lee and Sakthivel[12] proposed the Exp-function method to generate a rich class of traveling wave solutions. Using a extended mapping method and the availability of symbolic computation, several classes of exact solutions are expressed by various JEFs and hyperbolic functions.[13] Wu and Liu[14] found two types of nonlinear wave solutions called compacton-like wave and kink-like wave solutions. The hyperbolic function solutions and the trigonometric function solutions with free parameters have been obtained in Ref. [15] using the G'/G-expansion method. Giresunlu *et al.*[16] obtained exact traveling wave solutions using Lie symmetry analysis together with the simplest equation method and the Kudryashov method, and constructed exact solutions using the conservation laws and symmetries of the underlying equation. Some analytical solutions are given in Ref. [17] using direct integration for negative and positive phase velocities. Applying the direct method and the method of elliptic ordinary differential equations, Kengne *et al.*[18] found some exact solutions and so forth.

There are some interesting problems: How do solitary wave and periodic wave solutions depend on parameters of a system? Are there dynamical behaviors of solitary wave and periodic wave solutions to Eq. (1)? To our knowledge, these problems have not been considered before for Eq. (1). In this paper, we consider the existence and dynamical behaviors of the exact explicit solitary wave and periodic wave solutions to Eq. (1) in different regions of the parametric space. We also give all possible exact explicit parametric representations for solitary wave and periodic wave solutions to Eq. (1). The present results more completely answer the above problems and enrich the results of Refs. [11–18].

In order to study the dynamical behaviors and to obtain the exact explicit traveling solutions to Eq. (1), we use the transformation

$$u(x,t) = v^2(\xi), \quad \xi = x - ct, \tag{2}$$

where $-\infty < v(\xi) < +\infty$, and c $(c \neq 0)$ is the wave speed, to reduce Eq. (1) to the following ordinary differential equation (ODE):

$$2(\beta v^2 + \alpha v - c)vv' + \delta(v^2)''' = 0, \tag{3}$$

where the primes represent the derivatives with respect to ξ.

*Project supported by the National Natural Science Foundation of China (Grant No. 11461022).

†Corresponding author. E-mail: mengqhhu@126.com

© 2021 Chinese Physical Society and IOP Publishing Ltd

Integrating Eq. (3) once with respect to ξ, we have

$$2vv''+2(v')^2-(av^4+bv^3+kv^2+g)=0, \tag{4}$$

where $a=-\frac{\beta}{2\delta}$, $b=-\frac{2\alpha}{3\delta}$, $k=\frac{c}{\delta}$, and g is an integral constant.

Setting $y=\mathrm{d}v/\mathrm{d}\xi$, we can obtain the following planar dynamical system:

$$\frac{\mathrm{d}v}{\mathrm{d}\xi}=y,\quad \frac{\mathrm{d}y}{\mathrm{d}\xi}=\frac{av^4+bv^3+kv^2+g-2y^2}{2v}. \tag{5}$$

From Refs. [19–24], we know that a solitary wave solution to Eq. (4) corresponds to a homoclinic orbit of system (5), a peakon (or a periodic cusp wave) solution to Eq. (4) corresponds to a heteroclinic orbit (or the so-called connecting orbit) of system (5). Similarly, a periodic orbit of system (5) corresponds to a smooth periodic wave solution to Eq. (4). Thus, to investigate all possible solitary waves, peakons and periodic waves of Eq. (4), we need to find all homoclinic, heteroclinic and periodic annuli of system (5), which depend on the system parameters a,b,k and g. For simplicity, we only investigate the case of $a<0$ in this paper. The case of $a>0$ can be considered similarly, we omit it here.

2. Bifurcation sets and phase portraits of system (5)

Using the transformation $\mathrm{d}\xi=2v\mathrm{d}\tau$, we obtain the associated Hamiltonian system of system (5)

$$\frac{\mathrm{d}v}{\mathrm{d}\tau}=2vy,\quad \frac{\mathrm{d}y}{\mathrm{d}\tau}=av^4+bv^3+kv^2+g-2y^2. \tag{6}$$

System (6) has the following first integral:

$$H(v,y)=v^2\left[y^2-\left(\frac{a}{6}v^4+\frac{b}{5}v^3+\frac{k}{4}v^2+\frac{g}{2}\right)\right]=h. \tag{7}$$

For a fixed h, the level curve $H(v,y)=h$ defined by Eq. (7) determines a set of invariant curves of system (6), which contains different branches of curves. As h varies, it defines different families of orbits of system (6) with different dynamical behaviors.

Let

$$f_0(v)=av^4+bv^3+kv^2,\quad f(v)=av^4+bv^3+kv^2+g,$$

then we have

$$f(v)=f_0(v)+g,\quad f_0'(v)=v(4av^2+3bv+2k),$$
$$f_0''(v)=12av^2+6bv+2k.$$

Obviously, $f_0'(v)$ has the following zero points:

$$v_0=0,\quad v_\pm=\frac{-3b\pm\sqrt{\Delta_1}}{8a},$$

where $\Delta_1=9b^2-32ak$. Additionally,

$$f_0(v_0)=0,$$
$$f_0(v_+)=\frac{(-3b^2+b\sqrt{\Delta_1}+16ak)(3b-\sqrt{\Delta_1})^2}{2048a^3},$$
$$f_0(v_-)=\frac{(-3b^2-b\sqrt{\Delta_1}+16ak)(3b+\sqrt{\Delta_1})^2}{2048a^3},$$
$$f_0''(0)=2k,\quad f_0''(v_\pm)=\frac{\Delta_1\mp3b\sqrt{\Delta_1}}{8a}.$$

Moreover, $f_0(v_\pm)=0$, $f_0''(0)=0$ and $f_0''(v_\pm)=0$ imply that $k=\frac{b^2}{4a}$, $k=0$ and $k=\frac{9b^2}{32a}$, respectively.

Clearly, $(v_e,0)$ is a equilibrium point of system (6) if and only if $f(v_e)=0$. In other words, the equilibrium point $(v_e,0)$ of system (6) is just the intersection point of the straight line $z=-g$ and the curve defined by $z=f_0(v)$. From the above results and analyses of signs of $f_0''(0)$ and $f_0''(v_\pm)$, we can confirm the numbers and relative positions of equilibrium points of system (6) on the v-axis under different parameter conditions. On the other hand, it is easy to see that if $g>0$, then system (6) has two equilibrium points $(0,Y_\pm)$ on the line $v=0$, where $Y_\pm=\pm\frac{1}{2}\sqrt{2g}$.

Let $M(v_e,y_e)$ be the coefficient matrix of the linearized system of Eq. (6) at equilibrium point (v_e,y_e) and $J(v_e,y_e)=\det(M(v_e,y_e))$, we have

$$J(v_e,0)=-2v_ef_0'(v_e),\quad J(0,Y_\pm)=-8Y_\pm^2.$$

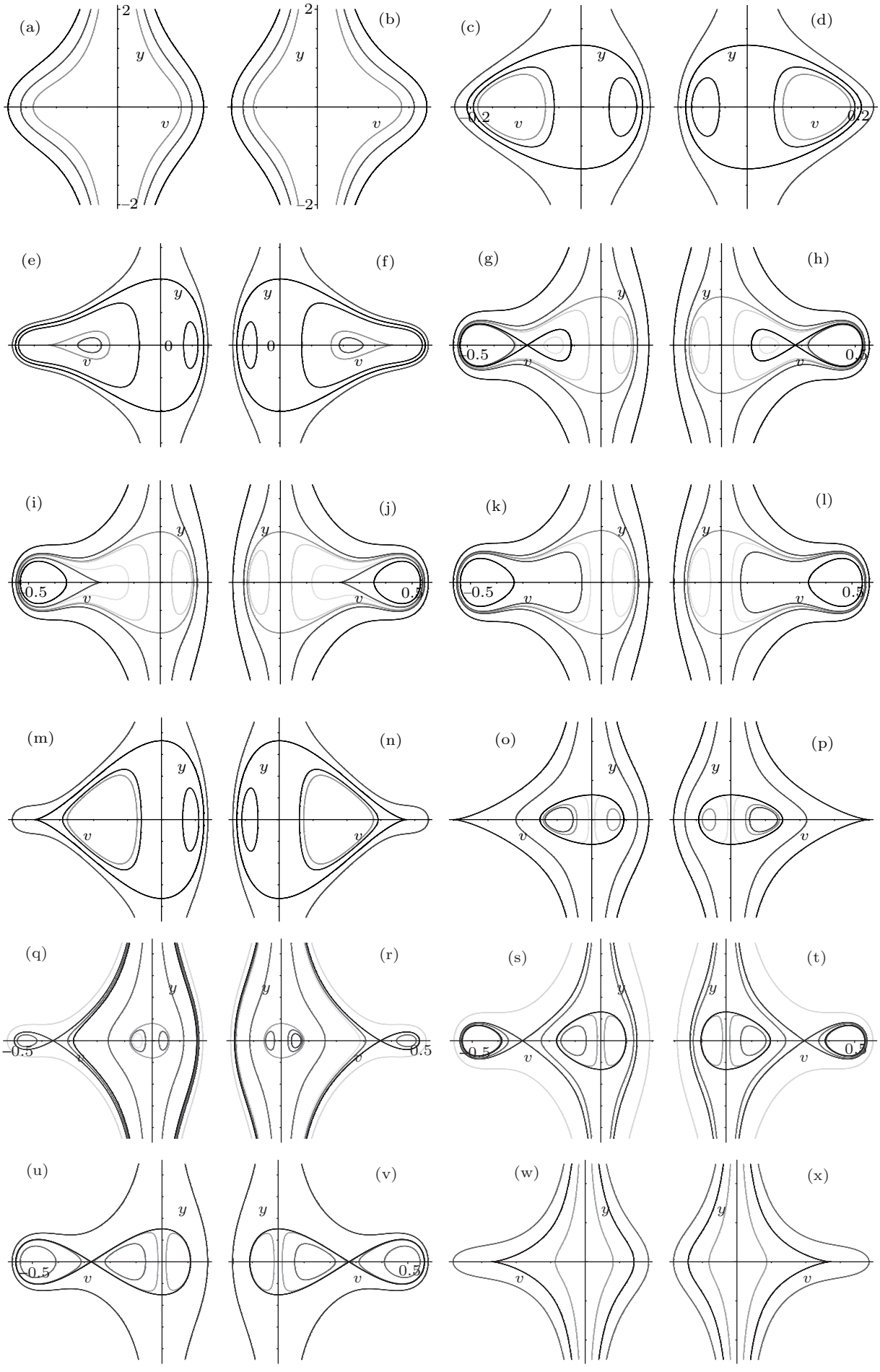
For an equilibrium point (v_e,y_e) of system (6), we know that (v_e,y_e) is a saddle point if $J(v_e,y_e)<0$, a center point if $J(v_e,y_e)>0$, a cusp if $J(v_e,y_e)=0$ and the Poincaré index of (v_e,y_e) is zero.

For fixed a and b, using the properties of the equilibrium points and the approach of dynamical system,[19–24] we can obtain the following bifurcation curves of system (6):

$$C_1:\ g=0,\quad C_2:\ g=-f_0(v_-),\quad C_3:\ g=-f_0(v_+),$$
$$C_4:\ g=\frac{3}{20000a^3}\left(243b^4-1350ab^2k+1250a^2k^2+(100abk-27b^3)\sqrt{\Delta_2}\right)\equiv g^*,$$
$$g=\frac{3}{20000a^3}\left(243b^4-1350ab^2k+1250a^2k^2-(100abk-27b^3)\sqrt{\Delta_2}\right)\equiv g^*,$$

which divide the (k,g)-parameter plane into different subregions, where $\Delta_2=81b^2-300ak$ and $\Delta_2=0$ implies $k=\frac{27b^2}{100a}$.

Since both systems (5) and (6) have the same first integral (7), the two systems have the same topological phase portraits except the straight line $v=0$. Therefore we can obtain the bifurcation sets and phase portraits of system (5) from those of system (6).


(a)
(b)
(c)
(d)
(e)
(f)
(g)
(h)
(i)
(j)
(k)
(l)
(m)
(n)
(o)
(p)
(q)
(r)
(s)
(t)
(u)
(v)
(w)
(x)
y
v
2
−2
0
0.2
−0.2
0.5
−0.5

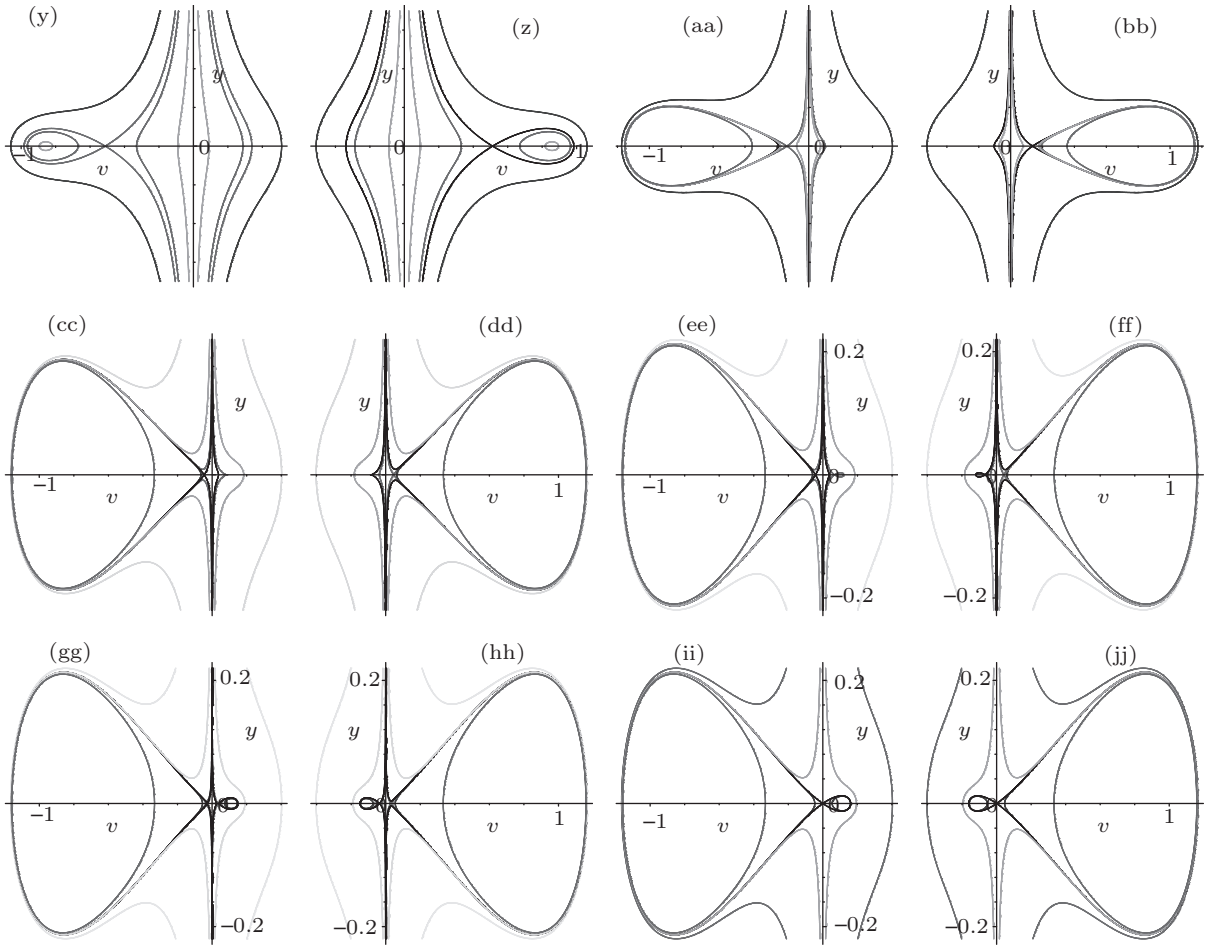


Fig. 1. Bifurcation sets and phase portraits of system (5) when $a<0$. Parameters: (a) $(k,b,g)\in A_1$. (b) $(k,b,g)\in A_2$. (c) $(k,b,g)\in A_3$. (d) $(k,b,g)\in A_4$. (e) $(k,b,g)\in A_5$. (f) $(k,b,g)\in A_6$. (g) $(k,b,g)\in A_7$. (h) $(k,b,g)\in A_8$. (i) $(k,b,g)\in A_9$. (j) $(k,b,g)\in A_{10}$. (k) $(k,b,g)\in A_{11}$. (l) $(k,b,g)\in A_{12}$. (m) $(k,b,g)\in A_{13}$. (n) $(k,b,g)\in A_{14}$. (o) $(k,b,g)\in A_{15}$. (p) $(k,b,g)\in A_{16}$. (q) $(k,b,g)\in A_{17}$. (r) $(k,b,g)\in A_{18}$. (s) $(k,b,g)\in A_{19}$. (t) $(k,b,g)\in A_{20}$. (u) $(k,b,g)\in A_{21}$. (v) $(k,b,g)\in A_{22}$. (w) $(k,b,g)\in A_{23}$. (x) $(k,b,g)\in A_{24}$. (y) $(k,b,g)\in A_{25}$. (z) $(k,b,g)\in A_{26}$. (aa) $(k,b,g)\in A_{27}$. (bb) $(k,b,g)\in A_{28}$. (cc) $(k,b,g)\in A_{29}$. (dd) $(k,b,g)\in A_{30}$. (ee) $(k,b,g)\in A_{31}$. (ff) $(k,b,g)\in A_{32}$. (gg) $(k,b,g)\in A_{33}$. (hh) $(k,b,g)\in A_{34}$. (ii) $(k,b,g)\in A_{35}$. (jj) $(k,b,g)\in A_{36}$.

Let

$$A_1=\left\{(k,b,g)|k<\frac{b^2}{4a},b<0,g\le 0\right\}\bigcup\left\{(k,b,g)|k=\frac{b^2}{4a},b<0,g<0\right\}\bigcup\left\{(k,b,g)|k>\frac{b^2}{4a},b<0,g<-f_0(v_+)\right\},$$

$$A_2=\left\{(k,b,g)|k<\frac{b^2}{4a},b>0,g\le 0\right\}\bigcup\left\{(k,b,g)|k=\frac{b^2}{4a},b>0,g<0\right\}\bigcup\left\{(k,b,g)|k>\frac{b^2}{4a},b>0,g<-f_0(v_-)\right\},$$

$$A_3=\left\{(k,b,g)|k\le\frac{9b^2}{32a},b<0,g>0\right\}\bigcup\left\{(k,b,g)|\frac{9b^2}{32a}<k<\frac{b^2}{4a},b<0,0<g<-f_0(v_+)\right\},$$

$$A_4=\left\{(k,b,g)|k\le\frac{9b^2}{32a},b>0,g>0\right\}\bigcup\left\{(k,b,g)|\frac{9b^2}{32a}<k<\frac{b^2}{4a},b>0,0<g<-f_0(v_-)\right\},$$

$$A_5=\left\{(k,b,g)|\frac{9b^2}{32a}<k<\frac{27b^2}{100a},b<0,g=-f_0(v_+)\right\},\quad A_6=\left\{(k,b,g)|\frac{9b^2}{32a}<k<\frac{27b^2}{100a},b>0,g=-f_0(v_-)\right\},$$

$$A_7=\left\{(k,b,g)|\frac{9b^2}{32a}<k\le\frac{27b^2}{100a},b<0,-f_0(v_+)<g<-f_0(v_-)\right\}\bigcup\left\{(k,b,g)|\frac{27b^2}{100a}<k<0,b<0,g^*<g<-f_0(v_-)\right\},$$

$$A_8=\left\{(k,b,g)|\frac{9b^2}{32a}<k\le\frac{27b^2}{100a},b>0,-f_0(v_-)<g<-f_0(v_+)\right\}\bigcup\left\{(k,b,g)|\frac{27b^2}{100a}<k<0,b>0,g^*<g<-f_0(v_+)\right\},$$

$$A_9=\left\{(k,b,g)|\frac{9b^2}{32a}<k<0,b<0,g=-f_0(v_-)\right\},\quad A_{10}=\left\{(k,b,g)|\frac{9b^2}{32a}<k<0,b>0,g=-f_0(v_+)\right\},$$

$$A_{11}=\left\{(k,b,g)|\frac{9b^2}{32a}<k<0,b<0,g>-f_0(v_-)\right\}\bigcup\{(k,b,g)|k>0,b<0,g>0\},$$

$$A_{12}=\left\{(k,b,g)|\frac{9b^2}{32a}<k<0,b>0,g>-f_0(v_+)\right\}\bigcup\{(k,b,g)|k>0,b>0,g>0\},$$

$$A_{13}=\{(k,b,g)|k=\frac{27b^2}{100a},b<0,g=-\frac{729b^4}{160000a^3}\},\quad A_{14}=\{(k,b,g)|k=\frac{27b^2}{100a},b>0,g=-\frac{729b^4}{160000a^3}\},$$
$$A_{15}=\left\{(k,b,g)|\frac{27b^2}{100a}<k<\frac{b^2}{4a},b<0,g=-f_0(v_+)\right\},\quad A_{16}=\left\{(k,b,g)|\frac{27b^2}{100a}<k<\frac{b^2}{4a},b>0,g=-f_0(v_-)\right\},$$
$$A_{17}=\left\{(k,b,g)|\frac{27b^2}{100a}<k\le\frac{b^2}{4a},b<0,-f_0(v_+)<g\le g^*\right\},\quad A_{18}=\left\{(k,b,g)|\frac{27b^2}{100a}<k\le\frac{b^2}{4a},b>0,-f_0(v_-)<g\le g^*\right\},$$
$$A_{19}=\left\{(k,b,g)|\frac{27b^2}{100a}<k\le\frac{b^2}{4a},b<0,g^*<g<g^*\right\}\bigcup\left\{(k,b,g)|\frac{b^2}{4a}<k<0,b<0,0<g<g^*\right\},$$
$$A_{20}=\left\{(k,b,g)|\frac{27b^2}{100a}<k\le\frac{b^2}{4a},b>0,g^*<g<g^*\right\}\bigcup\left\{(k,b,g)|\frac{b^2}{4a}<k<0,b>0,0<g<g^*\right\},$$
$$A_{21}=\left\{(k,b,g)|\frac{27b^2}{100a}<k<0,b<0,g=g^*\right\},\quad A_{22}=\left\{(k,b,g)|\frac{27b^2}{100a}<k<0,b>0,g=g^*\right\},$$
$$A_{23}=\left\{(k,b,g)|\frac{b^2}{4a}\le k,b<0,g=-f_0(v_+)\right\},\quad A_{24}=\left\{(k,b,g)|\frac{b^2}{4a}\le k,b>0,g=-f_0(v_-)\right\},$$
$$A_{25}=\left\{(k,b,g)|\frac{b^2}{4a}<k,b<0,-f_0(v_+)<g\le g^*\right\},\quad A_{26}=\left\{(k,b,g)|\frac{b^2}{4a}<k,b>0,-f_0(v_-)<g\le g^*\right\},$$
$$A_{27}=\left\{(k,b,g)|\frac{b^2}{4a}<k<0,b<0,g^*<g\le 0\right\}\bigcup\{(k,b,g)|k>0,b<0,g^*<g<-f_0(v_-)\},$$
$$A_{28}=\left\{(k,b,g)|\frac{b^2}{4a}<k<0,b>0,g^*<g\le 0\right\}\bigcup\{(k,b,g)|k>0,b>0,g^*<g<-f_0(v_+)\},$$
$$A_{29}=\{(k,b,g)|k>0,b<0,g=-f_0(v_-)\},\quad A_{30}=\{(k,b,g)|k>0,b>0,g=-f_0(v_+)\},$$
$$A_{31}=\{(k,b,g)|k>0,b<0,-f_0(v_-)<g\le g^*\},\quad A_{32}=\{(k,b,g)|k>0,b>0,-f_0(v_+)<g\le g^*\},$$
$$A_{33}=\{(k,b,g)|k>0,b<0,g^*<g<0\},\quad A_{34}=\{(k,b,g)|k>0,b>0,g^*<g<0\},$$
$$A_{35}=\{(k,b,g)|k>0,b<0,g=0\},\quad A_{36}=\{(k,b,g)|k>0,b>0,g=0\},$$

we show that bifurcation sets and phase portraits of system (5) in Fig. 1.

3. Exact explicit solitary wave and periodic wave solutions to Eq. (1)

According to Fig. 1 and the approach of dynamical system,[19–24] we present some exact explicit solitary wave and periodic wave solutions to Eq. (1) as follows.

Proposition 3.1. When $a<0,(k,b,g)\in A_{13}$, Eq. (1) has one ω-shape solitary wave solution

$$u(x,t)=\left(\frac{\alpha_1+v_1\left(\omega_1(x-ct)\right)^2}{1+\left(\omega_1(x-ct)\right)^2}\right)^2, \tag{8}$$

one solitary wave solution

$$u(x,t)=\left(\frac{\alpha_1+v_1\left(\Omega_1+\omega_1|x-ct|\right)^2}{1+\left(\Omega_1+\omega_1|x-ct|\right)^2}\right)^2, \tag{9}$$

and one periodic wave solution

$$u(x,t)=\left(\frac{\alpha_1+v_1\left(\Omega_1-\omega_1|x-ct-2nT_1|\right)^2}{1+\left(\Omega_1-\omega_1|x-ct-2nT_1|\right)^2}\right)^2,$$
$$(2n-1)T_1<x-ct<(2n+1)T_1, \tag{10}$$

where $\alpha_1=\frac{3b}{20a}$, $v_1=-\frac{9b}{20a}$, $\omega_1=\frac{\alpha_1-v_1}{12}\sqrt{-6a}$, $\Omega_1=\sqrt{-\frac{\alpha_1}{v_1}}$, $T_1=\left|\frac{\Omega_1}{\omega_1}\right|$, $n=0,\pm1,\pm2,\ldots$.

Proof For given $h=0$ in Fig. 1(m), the level curve is shown in Fig. 2(a). From Fig. 2(a), we see that the graph defined by $H(v,y)=0$ consists of one homoclinic orbit and three heteroclinic orbits when $a<0,(k,b,g)\in A_{13}$, the homoclinic orbit connecting with the cusp $(v_1,0)$, the saddle points $(0,\pm Y_1)$ and passing through point $(\alpha_1,0)$, two of the heteroclinic orbits connecting with the cusp $(v_1,0)$ and the saddle points $(0,\pm Y_1)$, the other heteroclinic orbit connecting with the saddle points $(0,\pm Y_1)$ and passing through point $(\alpha_1,0)$, where $v_1=-\frac{9b}{20a},Y_1=\frac{27b^2\sqrt{-2a}}{800a^2},\alpha_1=\frac{3b}{20a}$. In (v,y)-plane, their expressions are, respectively,

$$y=\pm\frac{1}{6}(v-v_1)\sqrt{-6a(\alpha_1-v)(v-v_1)},\ v_1<v\le\alpha_1, \tag{11}$$
$$y=\pm\frac{1}{6}(v-v_1)\sqrt{-6a(\alpha_1-v)(v-v_1)},\ v_1<v\le 0, \tag{12}$$
$$y=\pm\frac{1}{6}(v-v_1)\sqrt{-6a(\alpha_1-v)(v-v_1)},\ 0\le v\le\alpha_1. \tag{13}$$

Substituting Eqs. (11)–(13) into $\mathrm{d}v/\mathrm{d}\xi=y$ and integrating them along the homoclinic orbit, the heteroclinic orbits, respectively, we have

$$\int_v^{\alpha_1}\frac{\mathrm{d}s}{(s-v_1)\sqrt{(\alpha_1-s)(s-v_1)}}=\frac{1}{6}\sqrt{-6a}|\xi|, \tag{14}$$

$$\int_{v}^{0}\frac{\mathrm{d}s}{(s-v_1)\sqrt{(\alpha_1-s)(s-v_1)}}=\frac{1}{6}\sqrt{-6a}|\xi|, \quad (15)$$

$$\int_{0}^{v}\frac{\mathrm{d}s}{(s-v_1)\sqrt{(\alpha_1-s)(s-v_1)}}=\frac{1}{6}\sqrt{-6a}|\xi|. \quad (16)$$

Letting $v\to\alpha_1$ in Eq. (16), we obtain

$$\int_{0}^{\alpha_1}\frac{\mathrm{d}s}{(s-v_1)\sqrt{(\alpha_1-s)(s-v_1)}}=\frac{1}{6}\sqrt{-6a}T_1. \quad (17)$$

Completing the integrals in Eqs. (14)–(17), we can obtain one solitary wave solution, one peakon solution and one periodic cusp wave solution to Eq. (4) as follows:

$$v(\xi)=\frac{\alpha_1+v_1(\omega_1\xi)^2}{1+(\omega_1\xi)^2}, \quad (18)$$

$$v(\xi)=\frac{\alpha_1+v_1(\Omega_1+\omega_1|\xi|)^2}{1+(\Omega_1+\omega_1|\xi|)^2}, \quad (19)$$

$$v(\xi)=\frac{\alpha_1+v_1(\Omega_1-\omega_1|\xi-2nT_1|)^2}{1+(\Omega_1-\omega_1|\xi-2nT_1|)^2},\quad (2n-1)T_1<\xi<(2n+1)T_1, \quad (20)$$

where $\omega_1=\frac{\alpha_1-v_1}{12}\sqrt{-6a}$, $\Omega_1=\sqrt{-\frac{\alpha_1}{v_1}}$, $T_1=\left|\frac{\Omega_1}{\omega_1}\right|$, $n=0,\pm1,\pm2,\ldots$.

From Eqs. (2), (18)–(20), we can obtain one ω-shape solitary wave solution, one solitary wave solution and one periodic wave solution to Eq. (1) as Eqs. (8)–(10), respectively.

The proof of Proposition 3.1 is completed.

Proposition 3.2. When $a<0,(k,b,g)\in A_{14}$, Eq. (1) has one ω-shape solitary wave solution as Eq. (8), one solitary wave solution

$$u(x,t)=\left(\frac{\alpha_1+v_1(\Omega_1-\omega_1|x-ct|)^2}{1+(\Omega_1-\omega_1|x-ct|)^2}\right)^2, \quad (21)$$

and one periodic wave solution

$$u(x,t)=\left(\frac{\alpha_1+v_1(\Omega_1+\omega_1|x-ct-2nT_1|)^2}{1+(\Omega_1+\omega_1|x-ct-2nT_1|)^2}\right)^2,\quad (2n-1)T_1<x-ct<(2n+1)T_1, \quad (22)$$

where $\alpha_1,v_1,\omega_1,\Omega_1,T_1,n$ are given in Proposition 3.1.

Proof For given $h=0$ in Fig. 1(n), the level curve is shown in Fig. 2(b). From Fig. 2(b), we see that the graph defined by $H(v,y)=0$ consists of one homoclinic orbit and three heteroclinic orbits when $a<0$, $(k,b,g)\in A_{14}$, the homoclinic orbit connecting with the cusp $(v_1,0)$, the saddle points $(0,\pm Y_1)$ and passing through point $(\alpha_1,0)$, two of the heteroclinic orbits connecting with the cusp $(v_1,0)$ and the saddle points $(0,\pm Y_1)$, the other heteroclinic orbit connecting with the saddle points $(0,\pm Y_1)$ and passing through point $(\alpha_1,0)$, where $v_1=-\frac{9b}{20a}$, $Y_1=\frac{27b^2\sqrt{-2a}}{800a^2}$, $\alpha_1=\frac{3b}{20a}$. In (v,y)-plane, their expressions are, respectively,

$$y=\pm\frac{1}{6}(v_1-v)\sqrt{-6a(v_1-v)(v-\alpha_1)},\quad \alpha_1\le v<v_1, \quad (23)$$

$$y=\pm\frac{1}{6}(v_1-v)\sqrt{-6a(v_1-v)(v-\alpha_1)},\quad 0\le v<v_1, \quad (24)$$

$$y=\pm\frac{1}{6}(v_1-v)\sqrt{-6a(v_1-v)(v-\alpha_1)},\quad \alpha_1\le v\le 0. \quad (25)$$

Substituting Eqs. (23)–(25) into $\mathrm{d}v/\mathrm{d}\xi=y$ and integrating them along the homoclinic orbit, the heteroclinic orbits, respectively, we have

$$\int_{\alpha_1}^{v}\frac{\mathrm{d}s}{(v_1-s)\sqrt{(v_1-s)(s-\alpha_1)}}=\frac{1}{6}\sqrt{-6a}|\xi|, \quad (26)$$

$$\int_{0}^{v}\frac{\mathrm{d}s}{(v_1-s)\sqrt{(v_1-s)(s-\alpha_1)}}=\frac{1}{6}\sqrt{-6a}|\xi|, \quad (27)$$

$$\int_{v}^{0}\frac{\mathrm{d}s}{(v_1-s)\sqrt{(v_1-s)(s-\alpha_1)}}=\frac{1}{6}\sqrt{-6a}|\xi|. \quad (28)$$

Letting $v\to\alpha_1$ in Eq. (28), we obtain

$$\int_{\alpha_1}^{0}\frac{\mathrm{d}s}{(v_1-s)\sqrt{(v_1-s)(s-\alpha_1)}}=\frac{1}{6}\sqrt{-6a}T_1. \quad (29)$$

Completing the integrals in Eqs. (26)–(29), we can obtain one solitary wave solution to Eq. (4) as Eq. (18), one peakon solution and one periodic cusp wave solution to Eq. (4) as follows:

$$v(\xi)=\frac{\alpha_1+v_1(\Omega_1-\omega_1|\xi|)^2}{1+(\Omega_1-\omega_1|\xi|)^2}, \quad (30)$$

$$v(\xi)=\frac{\alpha_1+v_1(\Omega_1+\omega_1|\xi-2nT_1|)^2}{1+(\Omega_1+\omega_1|\xi-2nT_1|)^2},\quad (2n-1)T_1<\xi<(2n+1)T_1, \quad (31)$$

where $\omega_1=\frac{\alpha_1-v_1}{12}\sqrt{-6a}$, $\Omega_1=\sqrt{-\frac{\alpha_1}{v_1}}$, $T_1=\left|\frac{\Omega_1}{\omega_1}\right|$, $n=0,\pm1,\pm2,\ldots$.

From Eqs. (2), (18), (30) and (31), we can obtain one ω-shape solitary wave solution, one solitary wave solution and one periodic wave solution to Eq. (1) as Eqs. (8), (21) and (22), respectively.

The proof of Proposition 3.2 is completed.

Proposition 3.3. When $a<0,(k,b,g)\in A_{21}$, Eq. (1) has one ω-shape solitary wave solution

$$u(x,t)=\left(\frac{v_3\left(\alpha_2\cosh^2(\omega_2(x-ct))-\alpha_3\sinh^2(\omega_2(x-ct))\right)-\alpha_2\alpha_3}{\alpha_2\sinh^2(\omega_2(x-ct))-\alpha_3\cosh^2(\omega_2(x-ct))+v_3}\right)^2, \quad (32)$$

two solitary wave solutions

$$u(x,t)=\left(\frac{v_3\left(\alpha_2\sinh^2(\omega_2(x-ct))-\alpha_3\cosh^2(\omega_2(x-ct))\right)+\alpha_2\alpha_3}{\alpha_2\cosh^2(\omega_2(x-ct))-\alpha_3\sinh^2(\omega_2(x-ct))-v_3}\right)^2, \tag{33}$$

$$u(x,t)=\left(\frac{v_3\left(\mathrm{e}^{\Omega_2-2\omega_2|x-ct|}+(\alpha_2-\alpha_3)\right)^2-4\alpha_3(\alpha_2-v_3)\mathrm{e}^{\Omega_2-2\omega_2|x-ct|}}{\left(\mathrm{e}^{\Omega_2-2\omega_2|x-ct|}-(\alpha_2-\alpha_3)\right)^2+4(v_3-\alpha_3)\mathrm{e}^{\Omega_2-2\omega_2|x-ct|}}\right)^2, \tag{34}$$

and one periodic wave solution

$$u(x,t)=\left(\frac{v_3\left(\mathrm{e}^{\Omega_2+2\omega_2|x-ct-2nT_2|}+(\alpha_2-\alpha_3)\right)^2-4\alpha_3(\alpha_2-v_3)\mathrm{e}^{\Omega_2+2\omega_2|x-ct-2nT_2|}}{\left(\mathrm{e}^{\Omega_2+2\omega_2|x-ct-2nT_2|}-(\alpha_2-\alpha_3)\right)^2+4(v_3-\alpha_3)\mathrm{e}^{\Omega_2+2\omega_2|x-ct-2nT_2|}}\right)^2, \quad (2n-1)T_2<x-ct<(2n+1)T_2, \tag{35}$$

where

$$\omega_2=\frac{1}{12}\sqrt{-6a(\alpha_2-v_3)(v_3-\alpha_3)},\quad n=0,\pm1,\pm2,\ldots,\quad \Omega_2=\ln\left|\frac{2\alpha_2\alpha_3-v_3(\alpha_2+\alpha_3)+2\sqrt{-\alpha_2\alpha_3(\alpha_2-v_3)(v_3-\alpha_3)}}{v_3}\right|,$$

$$T_2=\frac{6}{\sqrt{-6a(\alpha_2-v_3)(v_3-\alpha_3)}}\ln\left|\frac{(\alpha_2-\alpha_3)v_3}{2\alpha_2\alpha_3-v_3(\alpha_2+\alpha_3)+2\sqrt{-2\alpha_2\alpha_3(\alpha_2-v_3)(v_3-\alpha_3)}}\right|,$$

v_1, v_2, v_3, v_4 $(v_4<v_3<v_2<v_1)$ are real roots of $(aX^2+bX+k)X^2+g^*=0$, α_2, α_3, v_3 satisfy $(X-\alpha_2)(X-v_3)^2(X-\alpha_3)=X^4+\frac{6b}{5a}X^3+\frac{3k}{2a}X^2+\frac{3g^*}{a}$.

Proof For given $h=0$ in Fig. 1(u), the level curve is shown in Fig. 2(c). From Fig. 2(c), we see that the graph defined by $H(v,y)=0$ consists of two homoclinic orbits and three heteroclinic orbits when $a<0,(k,b,g)\in A_{21}$, one of the homoclinic orbits connecting with the saddle points $(v_3,0),(0,\pm Y_2)$ and passing through point $(\alpha_2,0)$, the other homoclinic orbit connecting with the saddle point $(v_3,0)$ and passing through point $(\alpha_3,0)$, two of the heteroclinic orbits connecting with the saddle points $(v_3,0)$ and $(0,\pm Y_2)$, the other heteroclinic orbit connecting with the saddle points $(0,\pm Y_2)$ and passing through point $(\alpha_2,0)$, where v_3 is the second smallest real root of $(aX^2+bX+k)X^2+g^*=0, Y_2=\frac{1}{2}\sqrt{2g^*}$ and α_2,α_3,v_3 $(\alpha_3<v_3<\alpha_2)$ satisfy $(X-\alpha_2)(X-v_3)^2(X-\alpha_3)=X^4+\frac{6b}{5a}X^3+\frac{3k}{2a}X^2+\frac{3g^*}{a}$. In (v,y)-plane, their expressions are, respectively,

$$y=\pm\frac{1}{6}(v-v_3)\sqrt{-6a(\alpha_2-v)(v-\alpha_3)},\quad v_3<v\le\alpha_2, \tag{36}$$

$$y=\pm\frac{1}{6}(v_3-v)\sqrt{-6a(\alpha_2-v)(v-\alpha_3)},\quad \alpha_3\le v<v_3, \tag{37}$$

$$y=\pm\frac{1}{6}(v-v_3)\sqrt{-6a(\alpha_2-v)(v-\alpha_3)},\quad v_3<v\le 0, \tag{38}$$

$$y=\pm\frac{1}{6}(v-v_3)\sqrt{-6a(\alpha_2-v)(v-\alpha_3)},\quad 0\le v\le\alpha_2. \tag{39}$$

Substituting Eqs. (36)–(39) into $\mathrm{d}v/\mathrm{d}\xi=y$ and integrating them along the homoclinic orbits, the heteroclinic orbits, respectively, we have

$$\int_v^{\alpha_2}\frac{\mathrm{d}s}{(s-v_3)\sqrt{(\alpha_2-s)(s-\alpha_3)}}=\frac{1}{6}\sqrt{-6a}|\xi|, \tag{40}$$

$$\int_{\alpha_3}^{v}\frac{\mathrm{d}s}{(v_3-s)\sqrt{(\alpha_2-s)(s-\alpha_3)}}=\frac{1}{6}\sqrt{-6a}|\xi|, \tag{41}$$

$$\int_v^{0}\frac{\mathrm{d}s}{(s-v_3)\sqrt{(\alpha_2-s)(s-\alpha_3)}}=\frac{1}{6}\sqrt{-6a}|\xi|, \tag{42}$$

$$\int_0^{v}\frac{\mathrm{d}s}{(s-v_3)\sqrt{(\alpha_2-s)(s-\alpha_3)}}=\frac{1}{6}\sqrt{-6a}|\xi|. \tag{43}$$

Letting $v\to\alpha_2$ in Eq. (43), we obtain

$$\int_0^{\alpha_2}\frac{\mathrm{d}s}{(s-v_3)\sqrt{(\alpha_2-s)(s-\alpha_3)}}=\frac{1}{6}\sqrt{-6a}T_2. \tag{44}$$

Completing the integrals in Eqs. (40)–(44), we can obtain two solitary wave solutions, one peakon solution and one periodic cusp wave solution to Eq. (4) as follows:

$$v(\xi)=\frac{v_3\left(\alpha_2\cosh^2(\omega_2\xi)-\alpha_3\sinh^2(\omega_2\xi)\right)-\alpha_2\alpha_3}{\alpha_2\sinh^2(\omega_2\xi)-\alpha_3\cosh^2(\omega_2\xi)+v_3}, \tag{45}$$

$$v(\xi)=\frac{v_3\left(\alpha_2\sinh^2(\omega_2\xi)-\alpha_3\cosh^2(\omega_2\xi)\right)+\alpha_2\alpha_3}{\alpha_2\cosh^2(\omega_2\xi)-\alpha_3\sinh^2(\omega_2\xi)-v_3}, \tag{46}$$

$$v(\xi)=\frac{v_3\left(\mathrm{e}^{\Omega_2-2\omega_2|\xi|}+(\alpha_2-\alpha_3)\right)^2-4\alpha_3(\alpha_2-v_3)\mathrm{e}^{\Omega_2-2\omega_2|\xi|}}{\left(\mathrm{e}^{\Omega_2-2\omega_2|\xi|}-(\alpha_2-\alpha_3)\right)^2+4(v_3-\alpha_3)\mathrm{e}^{\Omega_2-2\omega_2|\xi|}}, \tag{47}$$

$$v(\xi)=\frac{v_3\left(\mathrm{e}^{\Omega_2+2\omega_2|\xi-2nT_2|}+(\alpha_2-\alpha_3)\right)^2-4\alpha_3(\alpha_2-v_3)\mathrm{e}^{\Omega_2+2\omega_2|\xi-2nT_2|}}{\left(\mathrm{e}^{\Omega_2+2\omega_2|\xi-2nT_2|}-(\alpha_2-\alpha_3)\right)^2+4(v_3-\alpha_3)\mathrm{e}^{\Omega_2+2\omega_2|\xi-2nT_2|}}, \quad (2n-1)T_2<\xi<(2n+1)T_2, \tag{48}$$

where

$$\omega_2=\frac{1}{12}\sqrt{-6a(\alpha_2-v_3)(v_3-\alpha_3)},\quad n=0,\pm1,\pm2,\ldots,\quad \Omega_2=\ln\left|\frac{2\alpha_2\alpha_3-v_3(\alpha_2+\alpha_3)+2\sqrt{-\alpha_2\alpha_3(\alpha_2-v_3)(v_3-\alpha_3)}}{v_3}\right|,$$

$$T_2=\frac{6}{\sqrt{-6a(\alpha_2-v_3)(v_3-\alpha_3)}}\ln\left|\frac{(\alpha_2-\alpha_3)v_3}{2\alpha_2\alpha_3-v_3(\alpha_2+\alpha_3)+2\sqrt{-2\alpha_2\alpha_3(\alpha_2-v_3)(v_3-\alpha_3)}}\right|.$$

From Eqs. (2), (45)–(48), we obtain one ω-shape solitary wave solution, two solitary wave solutions and one periodic wave solution to Eq. (1) as Eqs. (32)–(35), respectively.

The proof of Proposition 3.3 is completed.

Proposition 3.4. When $a<0,(k,b,g)\in A_{22}$, Eq. (1) has one ω-shape solitary wave solution

$$u(x,t)=\left(\frac{v_2\left(\alpha_4\sinh^2(\omega_3(x-ct))-\alpha_5\cosh^2(\omega_3(x-ct))\right)+\alpha_4\alpha_5}{\alpha_4\cosh^2(\omega_3(x-ct))-\alpha_5\sinh^2(\omega_3(x-ct))-v_2}\right)^2, \tag{49}$$

two solitary wave solutions

$$u(x,t)=\left(\frac{v_2\left(\alpha_4\cosh^2(\omega_3(x-ct))-\alpha_5\sinh^2(\omega_3(x-ct))\right)-\alpha_4\alpha_5}{\alpha_4\sinh^2(\omega_3(x-ct))-\alpha_5\cosh^2(\omega_3(x-ct))+v_2}\right)^2, \tag{50}$$

$$u(x,t)=\left(\frac{v_2\left(\mathrm{e}^{\Omega_3+2\omega_3|x-ct|}-(\alpha_4-\alpha_5)\right)^2+4\alpha_5(\alpha_4-v_2)\mathrm{e}^{\Omega_3+2\omega_3|x-ct|}}{\left(\mathrm{e}^{\Omega_3+2\omega_3|x-ct|}+(\alpha_4-\alpha_5)\right)^2-4(v_2-\alpha_5)\mathrm{e}^{\Omega_3+2\omega_3|x-ct|}}\right)^2, \tag{51}$$

and one periodic wave solution

$$u(x,t)=\left(\frac{v_2\left(\mathrm{e}^{\Omega_3-2\omega_3|x-ct-2nT_3|}-(\alpha_4-\alpha_5)\right)^2+4\alpha_5(\alpha_4-v_2)\mathrm{e}^{\Omega_3-2\omega_3|x-ct-2nT_3|}}{\left(\mathrm{e}^{\Omega_3-2\omega_3|x-ct-2nT_3|}+(\alpha_4-\alpha_5)\right)^2-4(v_2-\alpha_5)\mathrm{e}^{\Omega_3-2\omega_3|x-ct-2nT_3|}}\right)^2,\quad (2n-1)T_3<x-ct<(2n+1)T_3, \tag{52}$$

where

$$\omega_3=\frac{1}{12}\sqrt{-6a(\alpha_4-v_2)(v_2-\alpha_5)},\quad n=0,\pm1,\pm2,\ldots,\quad \Omega_3=\ln\left|\frac{v_2(\alpha_4+\alpha_5)-2\alpha_4\alpha_5+2\sqrt{-\alpha_4\alpha_5(\alpha_4-v_2)(v_2-\alpha_5)}}{v_2}\right|,$$

$$T_3=\frac{6}{\sqrt{-6a(\alpha_4-v_2)(v_2-\alpha_5)}}\ln\left|\frac{v_2(\alpha_4+\alpha_5)-2\alpha_4\alpha_5+2\sqrt{-2\alpha_4\alpha_5(\alpha_4-v_2)(v_2-\alpha_5)}}{(\alpha_4-\alpha_5)v_2}\right|,$$

α_4, α_5, v_2 satisfy $(X-\alpha_4)(X-v_2)^2(X-\alpha_5)=X^4+\frac{6b}{5a}X^3+\frac{3k}{2a}X^2+\frac{3g^*}{a}$.

Proof For given $h=0$ in Fig. 1(v), the level curve is shown in Fig. 2(d). From Fig. 2(d), we see that the graph defined by $H(v,y)=0$ consists of two homoclinic orbits and three heteroclinic orbits when $a<0,(k,b,g)\in A_{22}$, one of the homoclinic orbits connecting with the saddle points $(v_2,0),(0,\pm Y_3)$ and passing through point $(\alpha_5,0)$, the other homoclinic orbit connecting with the saddle point $(v_2,0)$ and passing through point $(\alpha_4,0)$, two of the heteroclinic orbits connecting with the saddle points $(v_2,0)$ and $(0,\pm Y_3)$, the other heteroclinic orbit connecting with the saddle points $(0,\pm Y_3)$ and passing through point $(\alpha_5,0)$, where v_2 is the second largest real root of $(aX^2+bX+k)X^2+g^*=0$, $Y_3=\frac{1}{2}\sqrt{2g^*}$ and α_4, α_5, v_2 $(\alpha_5<v_2<\alpha_4)$ satisfy $(X-\alpha_4)(X-\phi_2)^2(X-\alpha_5)=X^4+\frac{6b}{5a}X^3+\frac{3k}{2a}X^2+\frac{3g^*}{a}$. In (v,y)-plane, their expressions are, respectively,

$$y=\pm\frac{1}{6}(v_2-v)\sqrt{-6a(\alpha_4-v)(v-\alpha_5)},\quad \alpha_5\le v<v_2, \tag{53}$$

$$y=\pm\frac{1}{6}(v-v_2)\sqrt{-6a(\alpha_4-v)(v-\alpha_5)},\quad v_2<v\le\alpha_4, \tag{54}$$

$$y=\pm\frac{1}{6}(v_2-v)\sqrt{-6a(\alpha_4-v)(v-\alpha_5)},\quad 0\le v<v_2, \tag{55}$$

$$y=\pm\frac{1}{6}(v_2-v)\sqrt{-6a(\alpha_4-v)(v-\alpha_5)},\quad \alpha_5\le v\le 0. \tag{56}$$

Substituting Eqs. (53)–(56) into $\mathrm{d}v/\mathrm{d}\xi=y$ and integrating them along the homoclinic orbits, the heteroclinic orbits, respectively, we have

$$\int_{\alpha_5}^{v}\frac{\mathrm{d}s}{(v_2-s)\sqrt{(\alpha_4-s)(s-\alpha_5)}}=\frac{1}{6}\sqrt{-6a}|\xi|, \tag{57}$$

$$\int_{v}^{\alpha_4}\frac{\mathrm{d}s}{(s-v_2)\sqrt{(\alpha_4-s)(s-\alpha_5)}}=\frac{1}{6}\sqrt{-6a}|\xi|, \tag{58}$$

$$\int_0^v \frac{\mathrm{d}s}{(v_2-s)\sqrt{(\alpha_4-s)(s-\alpha_5)}} = \frac{1}{6}\sqrt{-6a}|\xi|, \tag{59}$$

$$\int_v^0 \frac{\mathrm{d}s}{(v_2-s)\sqrt{(\alpha_4-s)(s-\alpha_5)}} = \frac{1}{6}\sqrt{-6a}|\xi|. \tag{60}$$

Letting $v \to \alpha_5$ in Eq. (60), we obtain

$$\int_{\alpha_5}^0 \frac{\mathrm{d}s}{(v_2-s)\sqrt{(\alpha_4-s)(s-\alpha_5)}} = \frac{1}{6}\sqrt{-6a}T_3. \tag{61}$$

Completing the integrals in Eqs. (57)–(61), we can obtain two solitary wave solutions, one peakon solution and one periodic cusp wave solution to Eq. (4) as follows:

$$v(\xi) = \frac{v_2\left(\alpha_4\sinh^2(\omega_3\xi) - \alpha_5\cosh^2(\omega_3\xi)\right) + \alpha_4\alpha_5}{\alpha_4\cosh^2(\omega_3\xi) - \alpha_5\sinh^2(\omega_3\xi) - v_2}, \tag{62}$$

$$v(\xi) = \frac{v_2\left(\alpha_4\cosh^2(\omega_3\xi) - \alpha_5\sinh^2(\omega_3\xi)\right) - \alpha_4\alpha_5}{\alpha_4\sinh^2(\omega_3\xi) - \alpha_5\cosh^2(\omega_3\xi) + v_2}, \tag{63}$$

$$v(\xi) = \frac{v_2\left(\mathrm{e}^{\Omega_3+2\omega_3|\xi|} - (\alpha_4-\alpha_5)\right)^2 + 4\alpha_5(\alpha_4-v_2)\mathrm{e}^{\Omega_3+2\omega_3|\xi|}}{\left(\mathrm{e}^{\Omega_3+2\omega_3|\xi|} + (\alpha_4-\alpha_5)\right)^2 - 4(v_2-\alpha_5)\mathrm{e}^{\Omega_3+2\omega_3|\xi|}}, \tag{64}$$

$$v(\xi) = \frac{v_2\left(\mathrm{e}^{\Omega_3-2\omega_3|\xi-2nT_3|} - (\alpha_4-\alpha_5)\right)^2 + 4\alpha_5(\alpha_4-v_2)\mathrm{e}^{\Omega_3-2\omega_3|\xi-2nT_3|}}{\left(\mathrm{e}^{\Omega_3-2\omega_3|\xi-2nT_3|} + (\alpha_4-\alpha_5)\right)^2 - 4(v_2-\alpha_5)\mathrm{e}^{\Omega_3-2\omega_3|\xi-2nT_3|}}, \quad (2n-1)T_3 < \xi < (2n+1)T_3, \tag{65}$$

where

$$\omega_3 = \frac{1}{12}\sqrt{-6a(\alpha_4-v_2)(v_2-\alpha_5)}, n = 0, \pm1, \pm2, \ldots, \quad \Omega_3 = \ln\left|\frac{v_2(\alpha_4+\alpha_5) - 2\alpha_4\alpha_5 + 2\sqrt{-\alpha_4\alpha_5(\alpha_4-v_2)(v_2-\alpha_5)}}{v_2}\right|,$$

$$T_3 = \frac{6}{\sqrt{-6a(\alpha_4-v_2)(v_2-\alpha_5)}}\ln\left|\frac{v_2(\alpha_4+\alpha_5) - 2\alpha_4\alpha_5 + 2\sqrt{-2\alpha_4\alpha_5(\alpha_4-v_2)(v_2-\alpha_5)}}{(\alpha_4-\alpha_5)v_2}\right|.$$

From Eqs. (2), (62)–(65), we obtain one ω-shape solitary wave solution, two solitary wave solutions and one periodic wave solution to Eq. (1) as Eqs. (49)–(52), respectively.

The proof of Proposition 3.4 is completed.

Proposition 3.5. When $a<0$, $(k,b,g) \in A_{35}$ (or $a<0$, $(k,b,g) \in A_{36}$), Eq. (1) has two solitary wave solutions

$$u(x,t) = \left(\frac{\alpha_6\alpha_7}{\alpha_6\sinh^2(\omega_4(x-ct)) - \alpha_7\cosh^2(\omega_4(x-ct))}\right)^2, \tag{66}$$

$$u(x,t) = \left(\frac{\alpha_6\alpha_7}{\alpha_6\cosh^2(\omega_4(x-ct)) - \alpha_7\sinh^2(\omega_4(x-ct))}\right)^2. \tag{67}$$

Here, $\alpha_{6,7} = \frac{-6b\pm\sqrt{36b^2-150ak}}{10a}$, $\omega_4 = \frac{1}{12}\sqrt{6a\alpha_6\alpha_7}$.

Proof For given $h=0$ in Figs. 1(ii) and 1(jj), the level curves are shown in Figs. 2(e) and 2(f), respectively. From Figs. 2(e) and 2(f), we see that the graph defined by $H(v,y)=0$ consists of two homoclinic orbits when $a<0$, $(k,b,g) \in A_{35}$ (or $a<0, (k,b,g) \in A_{36}$), the homoclinic orbits connecting with the saddle point $(0,0)$ and passing through points $(\alpha_6,0),(\alpha_7,0)$, respectively, where $\alpha_{6,7} = \frac{-6b\pm\sqrt{36b^2-150ak}}{10a}$. In (v,y)-plane, their expressions are, respectively,

$$y = \pm\frac{1}{6}v\sqrt{-6a(\alpha_7-v)(v-\alpha_6)}, \ \alpha_6 \le v < 0, \tag{68}$$

$$y = \pm\frac{1}{6}v\sqrt{-6a(\alpha_7-v)(v-\alpha_6)}, \ 0 < v \le \alpha_7. \tag{69}$$

Substituting Eqs. (68) and (69) into $\mathrm{d}v/\mathrm{d}\xi = y$ and integrating them along the homoclinic orbits, respectively, we have

$$\int_{\alpha_6}^v \frac{\mathrm{d}s}{s\sqrt{(\alpha_7-s)(s-\alpha_6)}} = \frac{1}{6}\sqrt{-6a}|\xi|, \tag{70}$$

$$\int_v^{\alpha_7} \frac{\mathrm{d}s}{s\sqrt{(\alpha_7-s)(s-\alpha_6)}} = \frac{1}{6}\sqrt{-6a}|\xi|. \tag{71}$$

Completing the integrals in Eqs. (70) and (71), we can obtain two solitary wave solutions to Eq. (4) as follows:

$$v(\xi) = \frac{-\alpha_6\alpha_7}{\alpha_6\sinh^2(\omega_4\xi) - \alpha_7\cosh^2(\omega_4\xi)}, \tag{72}$$

$$v(\xi) = \frac{\alpha_6\alpha_7}{\alpha_6\cosh^2(\omega_4\xi) - \alpha_7\sinh^2(\omega_4\xi)}, \tag{73}$$

where $\omega_4 = \frac{1}{12}\sqrt{6a\alpha_6\alpha_7}$.

From Eqs. (2), (72) and (73), we obtain two solitary wave solutions to Eq. (1) as Eqs. (66) and (67).

The proof of Proposition 3.5 is completed.

Proposition 3.6. When $a<0, (k,b,g) \in A_{33}$ (or $a<0$, $(k,b,g) \in A_{34}$), Eq. (1) has two periodic wave solutions

$$u(x,t) = \left(\frac{\gamma_3(\gamma_4-\gamma_2) + \gamma_2(\gamma_3-\gamma_4)\mathrm{sn}^2(\omega_5(x-ct),k_1)}{(\gamma_4-\gamma_2) + (\gamma_3-\gamma_4)\mathrm{sn}^2(\omega_5(x-ct),k_1)}\right)^2, \tag{74}$$

$$u(x,t) = \left(\frac{\gamma_1(\gamma_2-\gamma_4) + \gamma_4(\gamma_1-\gamma_2)\mathrm{sn}^2(\omega_5(x-ct),k_1)}{(\gamma_2-\gamma_4) + (\gamma_1-\gamma_2)\mathrm{sn}^2(\omega_5(x-ct),k_1)}\right)^2, \tag{75}$$

where $\omega_5 = \frac{1}{12}\sqrt{-6a(\gamma_1-\gamma_3)(\gamma_2-\gamma_4)}$, $k_1 = \sqrt{\frac{(\gamma_1-\gamma_2)(\gamma_3-\gamma_4)}{(\gamma_1-\gamma_3)(\gamma_2-\gamma_4)}}$, $\gamma_1, \gamma_2, \gamma_3, \gamma_4$ $(\gamma_4 < \gamma_3 < \gamma_2 < \gamma_1)$ are real roots of $X^4 + \frac{6b}{5a}X^3 +$

$\frac{3k}{2a}X^2+\frac{3g}{a}=0$ and $\mathrm{sn}(\cdot,k)$ is the Jacobian elliptic function with the modulus k.[25,26]

Proof For given $h=0$ in Figs. 1(gg) and 1(hh), the level curves are shown in Figs. 2(g) and 2(h), respectively. From Figs. and 2(h), we see that the graph defined by $H(v,y)=0$ consists of two periodic orbits when $a<0$, $(k,b,g)\in A_{33}$ (or $a<0$, $(k,b,g)\in A_{34}$), one of them passing through points $(\gamma_4,0),(\gamma_3,0)$, and the other passing through points $(\gamma_2,0),(\gamma_1,0)$, where γ_1, γ_2, γ_3, γ_4 $(\gamma_4<\gamma_3<\gamma_2<\gamma_1)$ are real roots of $X^4+\frac{6b}{5a}X^3+\frac{3k}{2a}X^2+\frac{3g}{a}=0$. In (v,y)-plane, their expressions are, respectively,

$$y=\pm\frac{1}{6}\sqrt{-6a(\gamma_1-v)(\gamma_2-v)(\gamma_3-v)(v-\gamma_4)},\quad \gamma_4\le v\le\gamma_3, \tag{76}$$

$$y=\pm\frac{1}{6}\sqrt{-6a(\gamma_1-v)(v-\gamma_2)(v-\gamma_3)(v-\gamma_4)},\quad \gamma_2\le v\le\gamma_1. \tag{77}$$

Substituting Eqs. (76) and (77) into $\mathrm{d}v/\mathrm{d}\xi=y$ and integrating them along the periodic orbits, respectively, we have

$$\int_v^{\gamma_3}\frac{\mathrm{d}s}{\sqrt{(\gamma_1-s)(\gamma_2-s)(\gamma_3-s)(s-\gamma_4)}}=\frac{1}{6}\sqrt{-6a}|\xi|, \tag{78}$$

$$\int_v^{\gamma_1}\frac{\mathrm{d}s}{\sqrt{(\gamma_1-s)(s-\gamma_2)(s-\gamma_3)(s-\gamma_4)}}=\frac{1}{6}\sqrt{-6a}|\xi|. \tag{79}$$

Completing the integrals in Eqs. (78) and (79), we can obtain two periodic wave solutions to Eq. (4) as follows:

$$v(\xi)=\frac{\gamma_3(\gamma_4-\gamma_2)+\gamma_2(\gamma_3-\gamma_4)\mathrm{sn}^2(\omega_5\xi,k_1)}{(\gamma_4-\gamma_2)+(\gamma_3-\gamma_4)\mathrm{sn}^2(\omega_5\xi,k_1)}, \tag{80}$$

$$v(\xi)=\frac{\gamma_1(\gamma_2-\gamma_4)+\gamma_4(\gamma_1-\gamma_2)\mathrm{sn}^2(\omega_5\xi,k_1)}{(\gamma_2-\gamma_4)+(\gamma_1-\gamma_2)\mathrm{sn}^2(\omega_5\xi,k_1)}, \tag{81}$$

where $\omega_5=\frac{1}{12}\sqrt{-6a(\gamma_1-\gamma_3)(\gamma_2-\gamma_4)}$, $k_1=\sqrt{\frac{(\gamma_1-\gamma_2)(\gamma_3-\gamma_4)}{(\gamma_1-\gamma_3)(\gamma_2-\gamma_4)}}$ and $\mathrm{sn}(\cdot,k)$ is the Jacobian elliptic function with the modulus k.[25,26]

From Eqs. (2), (80) and (81), we obtain two periodic wave solutions to Eq. (1) as Eqs. (74) and (75).

The proof of Proposition 3.6 is completed.

Proposition 3.7. When $a<0$, $(k,b,g)\in A_{19}$, Eq. (1) has a periodic wave solution as Eq. (74). When $a<0$, $(k,b,g)\in A_{20}$, Eq. (1) has a periodic wave solution as Eq. (75).

Proof For given $h=0$ in Fig. 1(q), the level curve is shown in Fig. 2(i). From Fig. 2(i), we see that the graph defined by $H(v,y)=0$ consists of one periodic orbit and two heteroclinic orbits when $a<0$, $(k,b,g)\in A_{19}$, the periodic orbit passing through points $(\gamma_4,0),(\gamma_3,0)$, the heteroclinic orbits connecting with the saddle points $(0,\pm Y)$ and passing through points $(\gamma_2,0),(\gamma_1,0)$, respectively, where $Y=\frac{1}{2}\sqrt{2g},\gamma_1,\gamma_2,\gamma_3,\gamma_4$ $(\gamma_4<\gamma_3<\gamma_2<\gamma_1)$ are real roots of $X^4+\frac{6b}{5a}X^3+\frac{3k}{2a}X^2+\frac{3g}{a}=0$. In (v,y)-plane, their expressions are, respectively,

$$y=\pm\frac{1}{6}\sqrt{-6a(\gamma_1-v)(\gamma_2-v)(\gamma_3-v)(v-\gamma_4)},\quad \gamma_4\le v\le\gamma_3, \tag{82}$$

$$y=\pm\frac{1}{6}\sqrt{-6a(\gamma_1-v)(v-\gamma_2)(v-\gamma_3)(v-\gamma_4)},\quad \gamma_2\le v\le 0, \tag{83}$$

$$y=\pm\frac{1}{6}\sqrt{-6a(\gamma_1-v)(v-\gamma_2)(v-\gamma_3)(v-\gamma_4)},\quad 0\le v\le\gamma_1. \tag{84}$$

Substituting Eq. (82) into $\mathrm{d}v/\mathrm{d}\xi=y$ and integrating it along the periodic orbit, we have

$$\int_v^{\gamma_3}\frac{\mathrm{d}s}{\sqrt{(\gamma_1-s)(\gamma_2-s)(\gamma_3-s)(s-\gamma_4)}}=\frac{1}{6}\sqrt{-6a}|\xi|. \tag{85}$$

Completing the integral in Eq. (85), we can obtain one periodic wave solution to Eq. (4) as Eq. (80). From Eqs. (2) and (80), we obtain one periodic wave solution to Eq. (1) as Eq. (74).

For given $h=0$ in Fig. 1(r), the level curve is shown in Fig. 2(j). From Fig. 2(j), we see that the graph defined by $H(v,y)=0$ consists of two heteroclinic orbits and one periodic orbit when $a<0$, $(k,b,g)\in A_{20}$, the heteroclinic orbits connecting with the saddle points $(0,\pm Y)$ and passing through points $(\gamma_4,0),(\gamma_3,0)$, respectively, the periodic orbit passing through points $(\gamma_2,0)$, $(\gamma_1,0)$, where $Y=\frac{1}{2}\sqrt{2g}$, γ_1, γ_2, γ_3, γ_4 $(\gamma_4<\gamma_3<\gamma_2<\gamma_1)$ are real roots of $X^4+\frac{6b}{5a}X^3+\frac{3k}{2a}X^2+\frac{3g}{a}=0$. In (v,y)-plane, their expressions are, respectively,

$$y=\pm\frac{1}{6}\sqrt{-6a(\gamma_1-v)(\gamma_2-v)(\gamma_3-v)(v-\gamma_4)},\quad \gamma_4\le v\le 0, \tag{86}$$

$$y=\pm\frac{1}{6}\sqrt{-6a(\gamma_1-v)(\gamma_2-v)(\gamma_3-v)(v-\gamma_4)},\quad 0\le v\le\gamma_3, \tag{87}$$

$$y=\pm\frac{1}{6}\sqrt{-6a(\gamma_1-v)(v-\gamma_2)(v-\gamma_3)(v-\gamma_4)},\quad \gamma_2\le v\le\gamma_1. \tag{88}$$

Substituting Eq. (88) into $\mathrm{d}v/\mathrm{d}\xi=y$ and integrating it along the periodic orbit, we have

$$\int_v^{\gamma_1}\frac{\mathrm{d}s}{\sqrt{(\gamma_1-s)(s-\gamma_2)(s-\gamma_3)(s-\gamma_4)}}=\frac{1}{6}\sqrt{-6a}|\xi|. \tag{89}$$

Completing the integral in Eq. (89), we can obtain one periodic wave solution to Eq. (4) as Eq. (81). From Eqs. (2) and (81), we obtain one periodic wave solution to Eq. (1) as Eq. (75).

The proof of Proposition 3.7 is completed.

Proposition 3.8. When $a<0$, $(k,b,g)\in A_{27}$ (or $a<0$, $(k,b,g)\in A_{28}$ or $a<0,(k,b,g)\in A_{29}$ or $a<0$, $(k,b,g)\in A_{30}$ or $a<0$, $(k,b,g)\in A_{31}$ or $a<0$, $(k,b,g)\in A_{32}$), Eq. (1) has one periodic wave solution

$$u(x,t)=\left(\frac{\gamma_5B+\gamma_6A-(\gamma_5B-\gamma_6A)\mathrm{cn}(\omega_6(x-ct),k_2)}{B+A-(B-A)\mathrm{cn}(\omega_6(x-ct),k_2)}\right)^2, \tag{90}$$

where

$$\omega_6=\frac{1}{6G}\sqrt{-6a},\quad k_2=\sqrt{\frac{(\gamma_5-\gamma_6)^2-(A-B)^2}{4AB}},\quad A=\sqrt{(\gamma_5-b_1)^2+a_1^2},\quad B=\sqrt{(\gamma_6-b_1)^2+a_1^2},\quad G=\frac{1}{\sqrt{AB}},$$

γ_5, γ_6 $(\gamma_6<\gamma_5)$, a_1, b_1 satisfy $(X-\gamma_5)(X-\gamma_6)\left((X-b_1)^2+a_1^2\right)=X^4+\dfrac{6b}{5a}X^3+\dfrac{3k}{2a}X^2+\dfrac{3g}{a}$ and $\mathrm{cn}(\cdot,k)$ is the Jacobian elliptic function with the modulus k.[25,26]

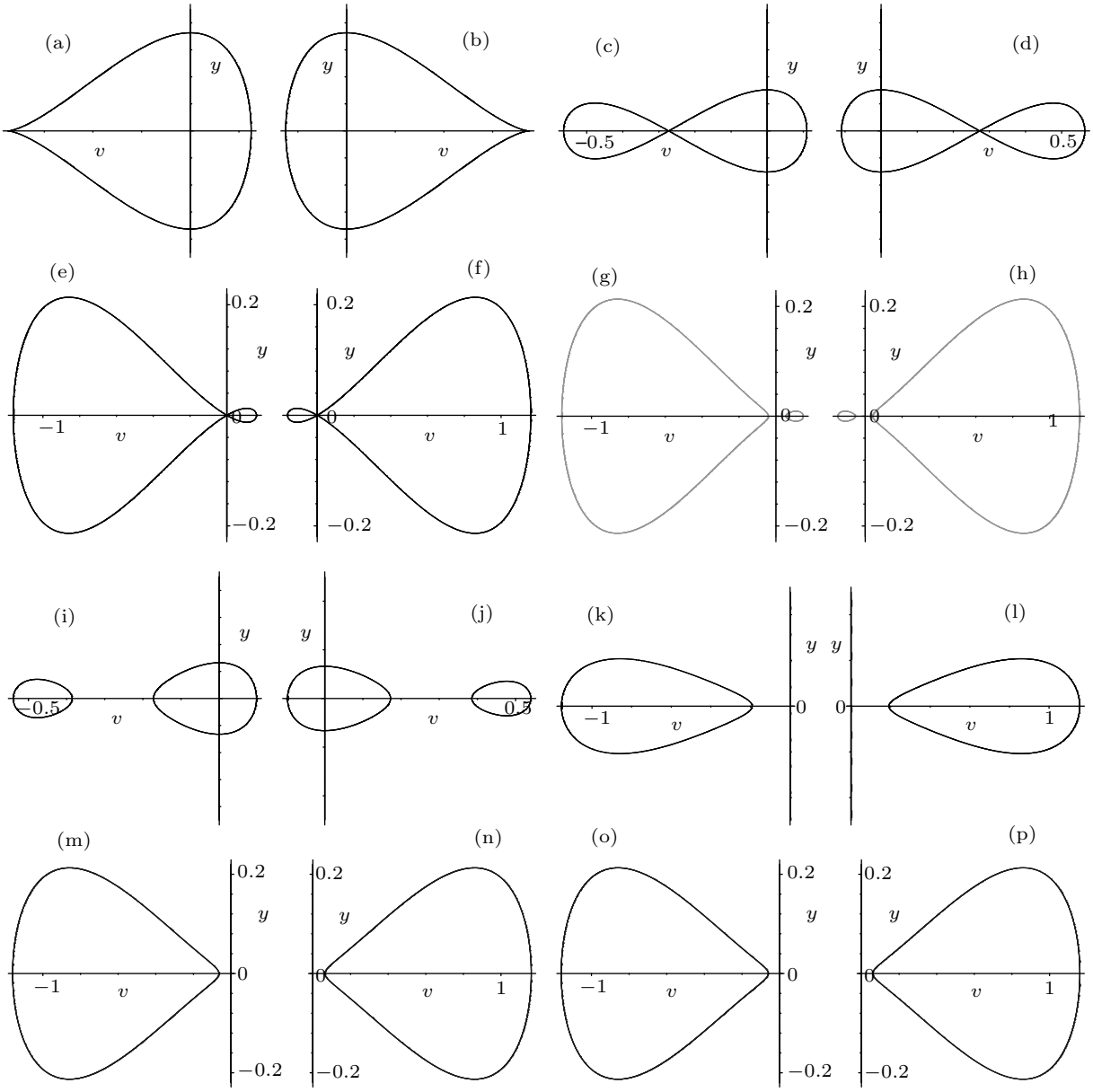


Fig. 2. The level curves defined by $H(v,y)=0$ when $a<0$. Parameters: (a) $(k,b,g)\in A_{13}$. (b) $(k,b,g)\in A_{14}$. (c) $(k,b,g)\in A_{21}$. (d) $(k,b,g)\in A_{22}$. (e) $(k,b,g)\in A_{35}$. (f) $(k,b,g)\in A_{36}$. (g) $(k,b,g)\in A_{33}$. (h) $(k,b,g)\in A_{34}$. (i) $(k,b,g)\in A_{19}$. (j) $(k,b,g)\in A_{20}$. (k) $(k,b,g)\in A_{27}$. (l) $(k,b,g)\in A_{28}$. (m) $(k,b,g)\in A_{29}$. (n) $(k,b,g)\in A_{30}$. (o) $(k,b,g)\in A_{31}$. (p) $(k,b,g)\in A_{32}$.

Proof For given $h=0$ in Figs. 1(aa)–1(ff), the level curves are shown in Figs. 2(k)–2(p), respectively. From Figs. 2(k)–2(p), we see that the graph defined by $H(v,y)=0$ consists of one periodic orbit when $a<0$, $(k,b,g)\in A_{27}$ (or $a<0$, $(k,b,g)\in A_{28}$ or $a<0,(k,b,g)\in A_{29}$ or $a<0$, $(k,b,g)\in A_{30}$ or $a<0,(k,b,g)\in A_{31}$ or $a<0$, $(k,b,g)\in A_{32}$), the periodic orbit passing through points $(\gamma_6,0),(\gamma_5,0)$. In (v,y)-plane, its expression is

$$y=\pm\frac{1}{6}\sqrt{-6a(\gamma_5-v)(v-\gamma_6)\left((v-b_1^2)^2+a_1^2\right)},\quad \gamma_6\le v\le\gamma_5, \tag{91}$$

where γ_5, γ_6 $(\gamma_6<\gamma_5)$, a_1, b_1 satisfy $(X-\gamma_5)(X-\gamma_6)\left((X-b_1)^2+a_1^2\right)=X^4+\frac{6b}{5a}X^3+\frac{3k}{2a}X^2+\frac{3g}{a}$.

Substituting Eq. (91) into $\mathrm{d}v/\mathrm{d}\xi=y$ and integrating it

along the periodic orbit, we have

$$\int_{\gamma_6}^{v} \frac{\mathrm{d}s}{\sqrt{(\gamma_5-s)(s-\gamma_6)\left((s-b_1^2)^2+a_1^2\right)}} = \frac{1}{6}\sqrt{-6a}|\xi|. \quad (92)$$

Completing the integral in Eq. (92), we can obtain one periodic wave solution to Eq. (4) as follows:

$$v(\xi) = \frac{\gamma_5 B+\gamma_6 A-(\gamma_5 B-\gamma_6 A)\mathrm{cn}(\omega_6\xi,k_2)}{B+A-(B-A)\mathrm{cn}(\omega_6\xi,k_2)}, \quad (93)$$

where $\omega_6 = \frac{1}{6G}\sqrt{-6a}$, $k_2 = \sqrt{\frac{(\gamma_5-\gamma_6)^2-(A-B)^2}{4AB}}$, $A = \sqrt{(\gamma_5-b_1)^2+a_1^2}$, $B = \sqrt{(\gamma_6-b_1)^2+a_1^2}$, $G = \frac{1}{\sqrt{AB}}$ and $\mathrm{cn}(\cdot,k)$ is the Jacobian elliptic function with the modulus k.[25,26]

From Eqs. (2) and (93), we obtain one periodic wave solution to Eq. (1) as Eq. (90).

The proof of Proposition 3.8 is completed.

4. Numerical simulations

In this section, we simulate the analytical results along with above details of the analysis.

Under the parameter conditions $a<0$, $(k,b,g)\in A_{13}$, we can draw the profiles of Eqs. (18)–(20) and Eqs. (8)–(10). For example, taking $a=-1.2$, $b=-1.5$, the profiles of Eqs. (18)–(20) and Eqs. (8)–(10) are shown in Figs. 3(a)–3(f), respectively.

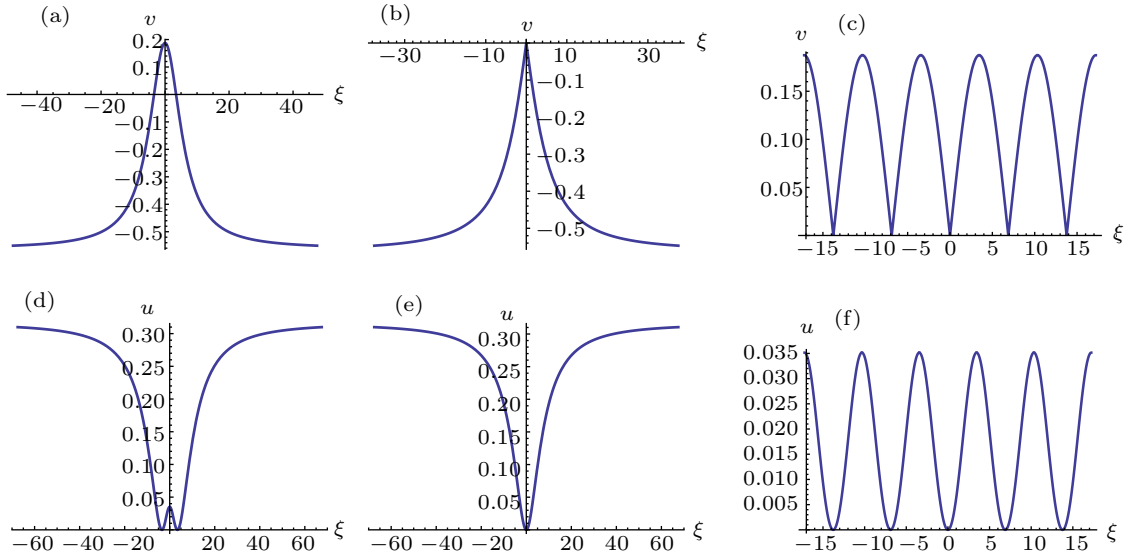


Fig. 3. Profiles of Eqs. (18)–(20) and Eqs. (8)–(10).

Under the parameter conditions $a<0$, $(k,b,g)\in A_{14}$, we can draw the profiles of Eqs. (18), (30), (31), (8), (21) and (22). For example, taking $a=-1.2$, $b=1.5$, the profiles of Eqs. (18), (30), (31), (8), (21) and (22) are shown in Figs. 4(a)–4(f), respectively.

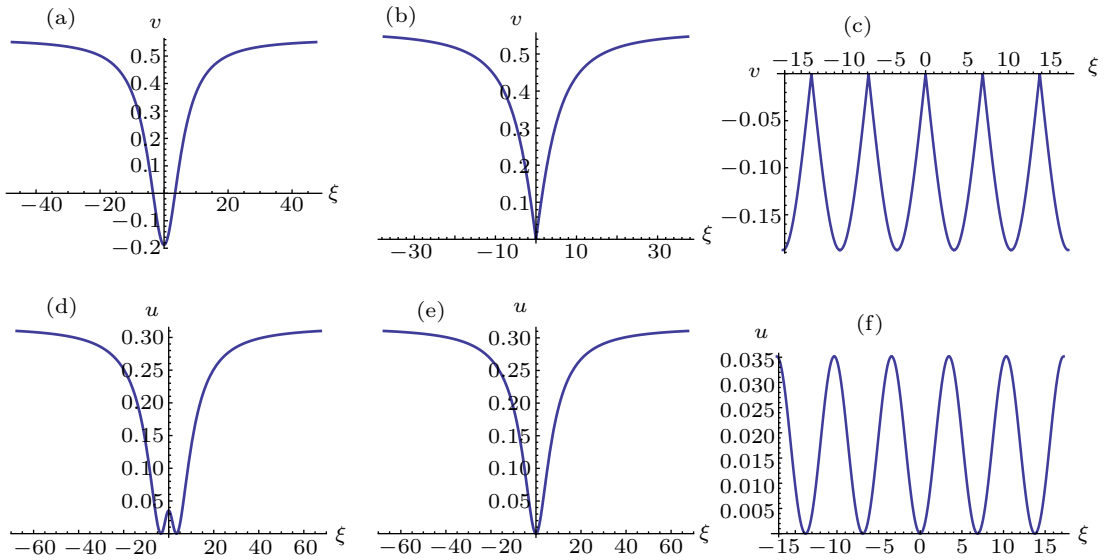


Fig. 4. Profiles of Eqs. (18), (30), (31), (8), (21) and (22).

Under the parameter conditions $a<0$, $(k,b,g)\in A_{21}$, we can draw the profiles of Eqs. (45)–(48) and Eqs. (32)–(35). For example, if $a=-2.0$, $b=-1.5$, then $\frac{27b^2}{100a}=-0.30375$. Taking $k=-0.29$, we have $\alpha_2\approx 0.1036828363$, $\alpha_3\approx -0.4722969027$, $v_3\approx -0.2656929669$, the profiles of Eqs. (45)–(48) and Eqs. (32)–(35) are shown in Figs. 5(a)–5(h), respectively.

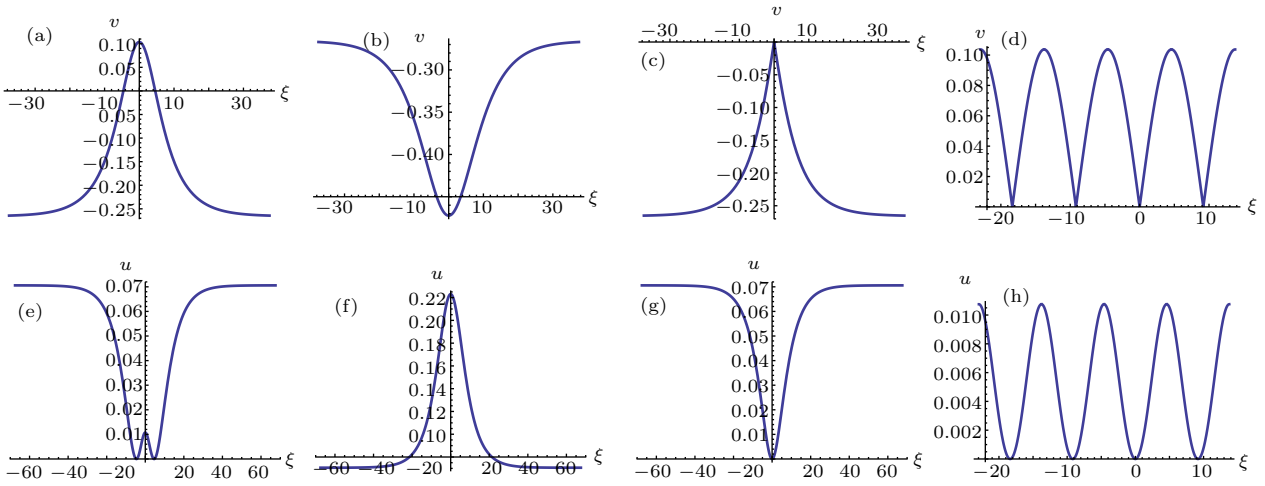


Fig. 5. Profiles of Eqs. (45)–(48) and Eqs. (32)–(35).

Under the parameter conditions $a<0$, $(k,b,g)\in A_{22}$, we can draw the profiles of Eqs. (62)–(65) and Eqs. (49)–(52). For example, if $a=-2.0$, $b=1.5$, then $\frac{27b^2}{100a}=-0.30375$. Taking $k=-0.29$, we have $\alpha_4\approx 0.4722969027$, $\alpha_5\approx -0.1036828363$, $v_2=0.2656929669$, the profiles of Eqs. (62)–(65) and Eqs. (49)–(52) are shown in Figs. 6(a)–6(h), respectively.

Under the parameter conditions $a<0$, $(k,b,g)\in A_{35}$ (or $a<0$, $(k,b,g)\in A_{36}$) we can draw the profiles of Eqs. (72), (73), (66) and (67). For example, taking $a=-1.5$, $b=-1.2$, $k=0.5$, the profiles of Eqs. (72), (73), (66), and (67) are shown in Figs. 7(a)–7(d), respectively.

Under the parameter conditions $a<0$, $(k,b,g)\in A_{33}$ (or $a<0$, $(k,b,g)\in A_{34}$ or $a<0$, $(k,b,g)\in A_{19}$), we can draw the profiles of Eqs. (80) and (74), and under the parameter conditions $a<0$, $(k,b,g)\in A_{33}$ (or $a<0$, $(k,b,g)\in A_{34}$ or $a<0$, $(k,b,g)\in A_{20}$), we can draw the profiles of Eqs. (81) and (75). For examples, if $a=-1.0$, $b=-1.2$, $k=0.2$, then $g^*\approx -0.0005436442500$. Taking $g=-0.0002$, we have $\gamma_1\approx 0.1735806979$, $\gamma_2\approx 0.05192544989$, $\gamma_3\approx -0.04097718240$, $\gamma_4\approx -1.624528965$, the profiles of Eqs. (80), (81), (74) and (75) are shown in Figs. 8(a), 8(b), 8(e), and 8(f), respectively. If $a=-1.2$, $b=-1.5$, then $\frac{27b^2}{100a}=-0.50625$, $\frac{b^2}{4a}=-0.46875$. Taking $k=-0.475$, we have $g^*\approx 0.006614208024$, $g^*\approx 0.009889698230$, and taking $g=0.008$, we have $\gamma_1\approx 0.1535974733$, $\gamma_2\approx -0.2834633650$, $\gamma_3\approx -0.5852607429$, $\gamma_4\approx -0.7848733654$, the profiles of Eqs. (80) and (74) are shown in Figs. 8(c) and 8(g), respectively. If $a=-0.5$, $b=1.5$, then $\frac{b^2}{4a}=-1.125$. Taking $k=-0.6$, we have $g^*\approx 0.01389438984$, and taking $g=0.007$, we have $\gamma_1\approx 3.001940363$, $\gamma_2\approx 0.5417948486$, $\gamma_3\approx 0.1912727276$, $\gamma_4\approx -0.1350079391$, the profiles of Eqs. (81) and (75) are shown in Figs. 8(d) and 8(h), respectively.

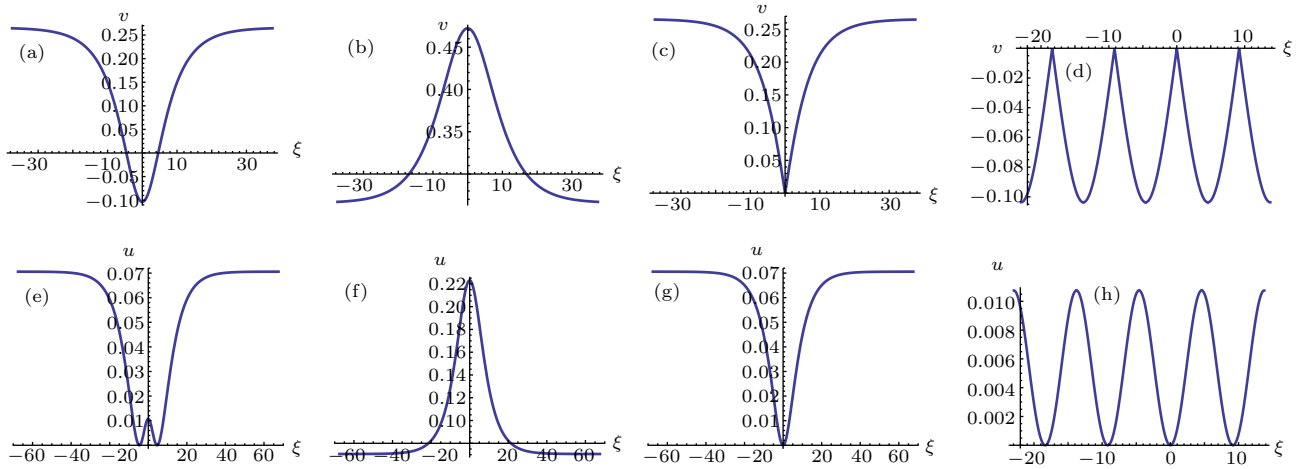


Fig. 6. Profiles of Eqs. (62)–(65) and Eqs. (49)–(52).

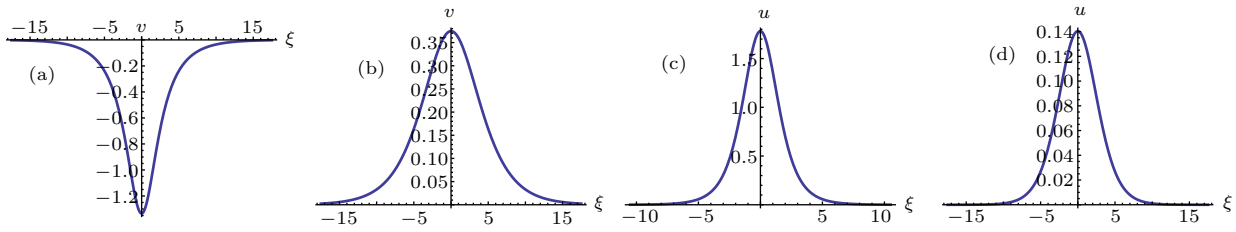


Fig. 7. Profiles of Eqs. (72), (73), (66), and (67).

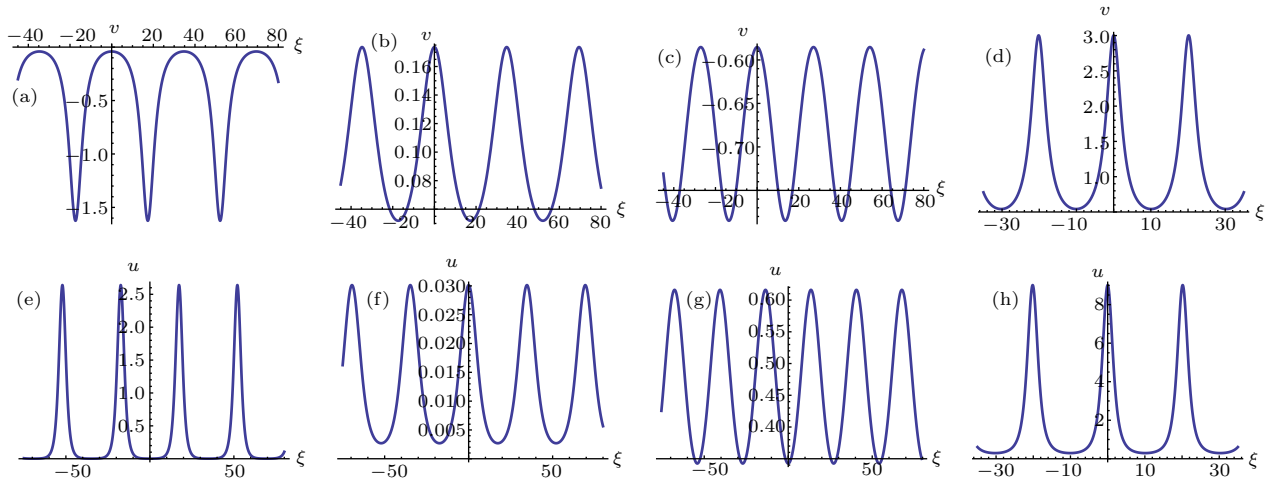


Fig. 8. Profiles of Eqs. (80), (81), (74) and (75).

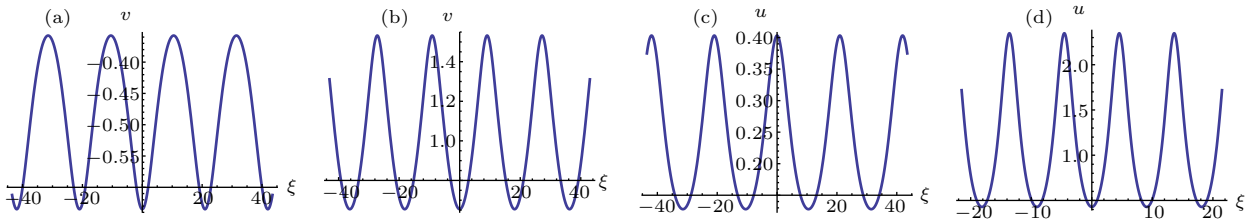


Fig. 9. Profiles of Eqs. (93) and (90).

Under the parameter conditions $a<0$, $(k,b,g)\in A_{27}$ (or $a<0$, $(k,b,g)\in A_{28}$ or $a<0$, $(k,b,g)\in A_{29}$ or $a<0$, $(k,b,g)\in A_{30}$ or $a<0$, $(k,b,g)\in A_{31}$ or $a<0$, $(k,b,g)\in A_{32}$), we can draw the profiles of Eqs. (93) and (90). For examples, if $a=-1.5$, $b=-1.0$, then $\frac{b^2}{4a}\approx -0.1666666667$. Taking $k=-0.08$, we have $g^*\approx -0.008872135956$, and taking $g=-0.005$, we have $\gamma_5\approx -0.3575950987$, $\gamma_6\approx -0.6349360676$, $a_1\approx 0.1864834974$, $b_1\approx 0.09626558315$, the profiles of Eqs. (93) and (90) are shown in Figs. 9(a) and 9(c), respectively. If $a=-1.2$, $b=1.1$, $k=0.7$, then $g^*\approx -0.4349753488$, $g^*\approx -0.01813511988$. Taking $g=-0.2$, we have $\gamma_5\approx 1.532083190$, $\gamma_6\approx 0.6546891617$, $a_1\approx 0.4507958913$, $b_1\approx -0.5433861760$, the profiles of Eqs. (93) and (90) are shown in Figs. 9(b) and 9(d), respectively.

5. Conclusion

In summary, we have investigated the existences and dynamical behaviors of exact explicit solitary wave and periodic wave solutions of the Schamel–Korteweg–de Vries equation (1) in different regions of the parametric space. Some exact explicit solitary wave and periodic wave solutions to Eq. (1) when $a<0,(k,b,g)\in A_{13}$ (or $a<0,(k,b,g)\in A_{14}$ or $a<0,(k,b,g)\in A_{21}$ or $a<0,(k,b,g)\in A_{22}$ or $a<0,(k,b,g)\in A_{35}$ or $a<0,(k,b,g)\in A_{36}$ or $a<0,(k,b,g)\in A_{33}$ or $a<0,(k,b,g)\in A_{34}$ or $a<0,(k,b,g)\in A_{19}$ or $a<0,(k,b,g)\in A_{20}$ or $a<0,(k,b,g)\in A_{27}$ or $a<0,(k,b,g)\in A_{28}$ or $a<0,(k,b,g)\in A_{29}$ or $a<0,(k,b,g)\in A_{30}$ or $a<0,(k,b,g)\in A_{31}$ or $a<0,(k,b,g)\in A_{32}$) are given in Propositions 3.1–3.8. Comparing with the results of [11–18], we obtain some new traveling wave solutions such as ω-shape solitary wave solutions (8), (32), (49), solitary wave solutions (9), (21), (34), (51), and periodic wave solutions (10), (22), (35), (52), etc. Obviously, there are still many works of Eq. (1) for studying in future, for examples, does the Eq. (1) exist loop soliton and periodic loop soliton solutions? How to obtain more non-traveling wave solutions to Eq. (1)? We will study Eq. (1) further.

References

[1] Gill T S, Bedi C and Saini N S 2011 *Phys. Plasmas* **18** 043701
[2] Mushtaq A, Khattak M N, Ahmad Z and Qamar A 2012 *Phys. Plasmas* **19** 042304
[3] Miura R M 1976 *SIAM Review* **18** 412
[4] Dodd R K, Eilbeck J C, Gibbon J D and Morris H C 1982 *Solitons and Nonlinear Wave Equations* (London: Academic Press)
[5] Schamel H 1972 *Plasma Phys.* **14** 905
[6] Schamel H and Shukla P K 1976 *Phys. Rev. Lett.* **36** 968
[7] El-Kalaawy O H 2011 *Phys. Plasmas* **18** 112302
[8] Ma W X and You Y C 2005 *Trans. Am. Math. Soc.* **357** 1753
[9] Ma W X 2015 *Phys. Lett. A* **379** 1975
[10] Ma W X and Zhou Y 2018 *J. Differ. Equations* **264** 2633
[11] Khater A H, Hassan M M and Temsah R S 2005 *J. Phys. Soc. Jpn.* **74** 1431
[12] Lee J and Sakthivel R 2011 *Rep. Math. Phys.* **68** 153
[13] Hassan M M 2010 *Commun. Theor. Phys.* **53** 596
[14] Wu Y and Liu Z R 2013 *Abstr. Appl. Anal.* **2013** 483492
[15] Kangalgil F 2016 *J. Egypt. Math. Soc.* **24** 526
[16] Giresunlu İ B, Sağlam Özkan Y and Yasar E 2017 *Math. Method Appl. Sci.* **40** 3927
[17] Daghan D and Donmez O 2018 *J. Appl. Mech. Tech. Phys.* **59** 389
[18] Kengne E, Lakhssassi A and Liu W M 2020 *Chaos Soliton Fract.* **140** 110229
[19] Li J B and Dai H H 2007 *On the Study of Singular Nonlinear Traveling Wave Equation: Dynamical System Approach* (Bejing: Science Press) (in Chinese)
[20] Li J B 2013 *Singular Nonlinear Traveling Wave Equations: Bifurcations and Exact Solutions* (Bejing: Science Press) (in Chinese)
[21] He B, Meng Q and Long Y 2012 *Commun. Nonlinear Sci. Numer. Simulat.* **17** 4137
[22] He B and Meng Q 2016 *Nonlinear Dyn.* **86** 811
[23] Li J B and Chen G R 2007 *Int. J. Bifur. Chaos* **17** 4049
[24] Li J B, Zhang Y and Zhao X H 2009 *Int. J. Bifur. Chaos* **19** 1995
[25] Byrd P F and Friedman M D 1971 *Handbook of Elliptic Integrals for Engineers and Physicists* (Berlin: Springer-Verlag)
[26] Chamdrasekharan K 1985 *Elliptic Functions* (Berlin: Springer-Verlag)